CAMBRIDGE
UNIVERSITY PRESS

Research Article

Dot to dot: High-z little red dots in $M_{\rm bh}$–$M_\star$ diagrams with galaxy-morphology-specific scaling relations

Alister W. Graham[1] , Igor Chilingarian[2,3] , Dieu Duc Nguyen[4], Roberto Soria[5,6] , Mark Durré[1] and Duncan A. Forbes[1]

[1]Centre for Astrophysics and Supercomputing, Swinburne University of Technology, Hawthorn, VIC, Australia, [2]Smithsonian Astrophysical Observatory, Cambridge, MA, USA, [3]Sternberg Astronomical Institute, M. V. Lomonosov Moscow State University, Moscow, Russia, [4]Simons Astrophysics Group (SAGI) at International Centre for Interdisciplinary Science and Education (ICISE), Institute For Interdisciplinary Research in Science and Education (IFIRST), Ghenh Rang, Quy Nhon, Vietnam, [5]INAF-Osservatorio Astrofisico di Torino, Pino Torinese, Italy and [6]Sydney Institute for Astronomy, School of Physics A28, The University of Sydney, Sydney, NSW, Australia

Abstract

The high redshift 'little red dots' (LRDs) detected with the *James Webb Space Telescope* are considered to be the cores of emerging galaxies that host active galactic nuclei (AGN). For the first time, we compare LRDs with local compact stellar systems and an array of galaxy-morphology-dependent stellar mass-black hole mass scaling relations in the $M_{\rm bh}$–$M_\star$ diagrams. When considering the 2023–2024 masses for LRDs, they are not equivalent to nuclear star clusters (NSCs), with the latter having higher $M_{\rm bh}/M_\star$ ratios. However, the least massive LRDs exhibit similar $M_{\rm bh}$ and $M_{\star,\rm gal}$ values as ultracompact dwarf (UCD) galaxies, believed to be the cores of stripped/threshed galaxies. We show that the LRDs span the $M_{\rm bh}$–$M_{\star,\rm gal}$ diagram from UCD galaxies to primaeval lenticular galaxies. In contrast, local spiral galaxies and the subset of major-merger-built early-type galaxies define $M_{\rm bh}$–$M_{\star,\rm gal}$ relations that are offset to higher stellar masses. Based on the emerging 2025 masses for LRDs, they may yet have similarities with NSCs, UCD galaxies, and green peas. Irrespective of this developing situation, we additionally observe that low-redshift galaxies with AGN align with the quasi-quadratic or steeper black hole scaling relations defined by local disc galaxies with directly measured black hole masses. This highlights the benefits of considering a galaxy's morphology – which reflects its accretion and merger history – to understand the coevolution of galaxies and their black holes. Future studies of spatially resolved galaxies with secure masses at intermediate-to-high redshift hold the promise of detecting the emergence and evolution of the galaxy-morphology-dependent $M_{\rm bh}$–$M_\star$ relations.

Keywords: Galaxies: bulges; galaxies: elliptical and lenticular; cD; galaxies: structure; galaxies: interactions; galaxies: evolution; (galaxies:) quasars: supermassive black holes

1. Introduction

After 3C 273 was determined to be receding at 1/6th the speed of light (redshift $z = 0.158$: Schmidt 1963), Schmidt's quasars have been found at ever-increasing redshifts. Izumi et al. (2021) report on over 40 low- and high-luminosity quasars[a] and quasi-stellar objects (QSOs) at $z \gtrsim 6$. While QSOs are predominantly blue, it was recognised that some dust-reddened active galactic nuclei (AGN) may have been overlooked in the past (e.g. Fall & Pei 1993; Webster et al. 1995; Stickel et al. 1996) and very high numbers are now being found. In addition to the samples of possible and confirmed AGN at $5 < z < 9$ (e.g. Harikane et al. 2023; Akins et al. 2024), recent records include an AGN at $z = 8.50$ (Kokorev et al. 2023), $z = 8.63$ (Tripodi et al. 2024), the QSO CEERS_1019 at $z = 8.7$ (Larson et al. 2023), and GNz11 (Maiolino et al. 2024, 2024;

Bunker et al. 2023). Due to their red rest-frame optical colour and compact appearance in *James Webb Space Telescope* (*JWST*) images,[b] some of these recently detected ($4 \lesssim z \lesssim 10$) red QSOs have been dubbed 'little red dots' (LRDs: Kocevski et al. 2023; Kokorev et al. 2023; Barro et al. 2024; Kocevski et al. 2025; Kokorev et al. 2024a; Matthee et al. 2024; Pérez-González et al. 2024; Yue et al. 2024)[c]

For years, it was reported (e.g. Bennert et al. 2011; Wang et al. 2013; Park et al. 2015; Venemans et al. 2016; Decarli et al. 2018; Ding et al. 2020; Pensabene et al. 2020) that high-z galaxies with AGN reside above the original $z \sim 0$ near-linear supermassive black hole (SMBH) mass – host spheroid stellar mass ($M_{\rm bh}$-$M_{\star,\rm sph}$) relation (Magorrian et al. 1998). This was regarded as evidence that, over time, the galaxies' stellar populations must play catch-up to the SMBHs for the systems to arrive at the $z \approx 0$ relation.

[a]Quasi-stellar radio sources (quasars) have strong radio emission, while QSOs do not.

[b]These nascent galaxies are sometimes spatially resolved (Rinaldi et al. 2024). However, a comparison of LRDs with UCD galaxies in the size-mass diagram is left for a follow-up paper once more LRD host galaxy sizes become available.

[c]Some LRDs, but more likely globular clusters, may have started life as the 'little blue dots' (LBDs) found by Elmegreen & Elmegreen (2017).

However, at least two factors were confounding the veracity of whether or not any evolution with redshift had been detected. The first was that the $z \sim 0$ $M_{\rm bh}$-$M_{\star}$ relation is not linear. For gas-rich systems, such as spiral (S) galaxies and (wet merger)-built lenticular (S0) galaxies, the $M_{\rm bh}$-$M_{\star}$ relation is much steeper than linear (Graham 2012; Graham & Scott 2013; Scott, Graham, & Schombert 2013). For the S galaxies, Savorgnan et al. (2016) presented the steep 'blue sequence' initially suggested by the data of Salucci et al. (2000) and subsequently better quantified by Davis et al. (2018, 2019). Selecting QSOs from massive gas-rich galaxies at high redshifts effectively samples the upper end of the steep non-linear relation and, therefore, samples from above the near-linear $z \sim 0$ relation. The apparent higher $M_{\rm bh}/M_{\star}$ ratios measured at higher redshift need not imply that there has been any evolution. This scenario can be appreciated by looking at (Izumi et al. 2021, their Figure 13) and (Kocevski et al. 2023, their Figure 9). These authors correctly noticed that the past trend with redshift in the $M_{\rm bh}$-$M_{\star}$ diagram was due to luminosity bias in past samples of high-z AGN. The explanation stems from the quadratic or steeper $M_{\rm bh}$-$M_{\star}$ relation.

The second issue has been the need for more attention to galaxy components and morphology. As stressed previously (e.g. Sahu, Graham, & Davis 2019), $M_{\rm bh}$-$M_{\star}$ scaling relations defined by grouping all galaxy types, or even just the early-type galaxies (ETGs), will be misleading. The slope and zero-point calibration of such relations will depend on the random number of specific galaxy types in one's sample. For example, the reported relations for samples of 'all ETGs' depend on the arbitrary fraction of primordial/primaeval[d] S0 galaxies (Graham 2023b) versus wet-major-merger-built S0 galaxies, the number of ellicular (ES)[e] and elliptical (E) galaxies, and the number of brightest cluster galaxies (BCGs) built from multiple major mergers. To fully address the topic of galaxy/black hole coevolution, one requires knowledge of the galaxy-morphology-dependent $M_{\rm bh}$-$M_{\star}$ relations that have progressively advanced over the last dozen years or so.

There is an additional population of ultracompact dwarf (UCD) galaxies (e.g. Harris, Pritchet, & McClure 1995; Hilker et al. 1999; Drinkwater et al. 2000; Phillipps et al. 2001; Madrid et al. 2010; Brodie et al. 2011; Chilingarian et al. 2011; Pfeffer & Baumgardt 2013; Forbes et al. 2020; Graham 2020) to consider. They are commonly thought to be the remnant nuclei of threshed low-mass disc galaxies (Zinnecker et al. 1988; Bekki, Couch, & Drinkwater 2001; Drinkwater et al. 2003), composed of the inner dense compact nuclear star cluster (NSC) from the progenitor galaxy and some residual galaxy stars forming a larger secondary component. Graham (2024b) suggested that LRDs might be somewhat akin to UCD galaxies with NSCs.[f] NSCs and the inner components of UCD galaxies occupy a similar distribution in the $M_{\rm bh}$−$M_{\star,{\rm sph}}$ diagram (Graham 2020). They are, however, often excluded from $M_{\rm bh}$−$M_{\star}$ scaling diagrams. This manuscript presents the central massive black hole mass versus the stellar mass

of NSCs, the inner component of UCD galaxies, the bulge component of disc galaxies, and the spheroidal component of E galaxies. It additionally displays black hole mass versus the total stellar mass of NSCs and UCD galaxies, along with all types of galaxies with directly measured black hole masses. Several samples of local AGN have also been added. Equipped with this background, we explore how LRDs compare.

Section 2 introduces the various data sets that appear in the $M_{\rm bh}$-$M_{\star,{\rm sph}}$ and $M_{\rm bh}$-$M_{\star,{\rm gal}}$ diagrams presented herein. Nearby galaxies with directly measured black hole masses, including UCD galaxies (Section 2.1.1), along with samples of low-z AGN (Section 2.2.1) and high-z AGN, including LRDs (Section 2.2.2), have representation. In Section 3, we discuss the $M_{\rm bh}$-$M_{\star}$ diagrams. We start with a short recap of developments over the past decade (Section 3.1), breaking away from the original near-linear relations (e.g. Dressler & Richstone 1988; Dressler 1989; Kormendy & Richstone 1995; Graham 2007, and references therein) defined by predominantly ETGs. In addition to advances using relations not based on one-fit-for-all types of galaxy, which are skewed/biased by the random fractions of ETGs and late-type galaxies (LTGs, i.e. S galaxies), in one's sample, we discuss how not grouping the different ETGs has similar benefits for avoiding a biased relation and revealing valuable scientific information. Section 3.2 discusses the LRDs and their distribution in the $M_{\rm bh}$-$M_{\star}$ diagrams. Finally, Section 3.3 describes the location of lower-z AGN in the diagrams, revealing that they follow the steep relations defined by local galaxies with predominantly inactive black holes. A concise summary is given in Section 4. Although almost all of the $z \approx 0$ galaxies and star clusters have had their masses obtained from redshift-independent distances, the slight differences in cosmologies between the studies of more distant AGN are ignored given that this will not account for the broad trends and no quantitative analysis is performed here.

2. Data

2.1. (Predominantly) inactive stellar systems

2.1.1. Galaxies with directly measured black hole masses

A local ($z \sim 0$) sample of predominantly inactive galaxies with directly measured SMBH masses is described in a recent series of papers spanning Graham & Sahu (2023a) to Graham (2024b). Multicomponent decompositions (Savorgnan & Graham 2016a; Davis et al. 2019; Sahu et al. 2019) of galaxy images obtained by the *Spitzer Space Telescope* (*SST*) were performed, separating inner discs (e.g. Scorza & van den Bosch 1998; Balcells, Graham, & Peletier 2007) and bar-induced (X/peanut shell)-shaped structures (e.g. de Vaucouleurs & de Vaucouleurs 1972; Ciambur & Graham 2016) from bulges. Bars, rings, and ansae were modelled. In addition to the single exponential disc model, truncated and anti-truncated disc models were used, as were inclined disc models as required.

The absence from the above sample of galaxies with (directly measured black hole masses and) $M_{\star,{\rm sph}} \lesssim 2 \times 10^9$ $M_{\odot}$ and $M_{\star,{\rm gal}} \lesssim 10^{10}$ $M_{\odot}$ is an observational bias due to difficulties measuring their central black hole mass. However, galaxies with lower stellar masses of course exist and are increasingly reported with directly measured SMBH masses. These additional galaxies are individually named in the diagrams and displayed with a different (cyan) symbol because they were not used to derive the scaling relations shown there.

---

[d]The term 'primaeval' is used here to refer to the first type of galaxy to form prior to subsequent significant merger events that change the galaxy type. This is expected to be a disc galaxy due to the conservation of angular momentum in the contracting gas clouds (Evrard, Summers, & Davis 1994), which need not but may be clumpy at high-z (Mowla, Iyer, & Asada 2024).

[e]Liller (1966) introduced the 'ES' galaxy nomenclature for ETGs with intermediate-scale discs that do not dominate the light at large radii. Graham et al. (2016b) introduced the name 'ellicular'.

[f]AWG discussed LRDs overlapping (connecting?) with UCD galaxies (and NSCs) at the July 2024 conferences http://cosmicorigins.space/smbh-sexten and https://indico.ict.inaf.it/event/2784/.

The ETGs were separated into BCGs, E and ES galaxies (Graham & Sahu 2023b), and S0 galaxies that were further separated into dust-poor and dust-rich, which is a good indicator of their origin as either primaeval (no major mergers, likely stripped of gas due to ram-pressure and thus 'preserved' but with an ageing stellar population)[g] or built from a wet major merger event likely involving an S galaxy (Graham 2023a,b). These latter dust-rich systems, presumably with considerable neutral hydrogen gas content, are also big galaxies with massive black holes that do not remove their gas on short timescales. For example, the dusty S0 galaxy Fornax A is a 3-Gyr-old merger product with $\sim 10^9$ M$_\odot$ of H I gas (Serra et al. 2019). However, not all major merger remnants have retained a dusty appearance.

In Graham (2024b), NGC 4697, NGC 3379, NGC 3091, and NGC 4649 were reclassified as S0 rather than E galaxies, with the adjustment supported by kinematic maps of the galaxies. Although not dust-rich, all but NGC 3091 – the brightest galaxy in Hickson Compact Group No. 42 – are recognised mergers in prior work. As detailed in Graham (2024b), their anti-truncated discs are also likely a signature of their merger origin. Two other S0 galaxies are regarded here as major-merger remnants, although they too are not classified (see Graham 2023a) as dust-rich (i.e. dust=Y, that is, a strong yes).[h] The first is NGC 5813[i] (dust=y, widespread but weak) (Hopp, Wagner, & Richtler 1995; Krajnović et al. 2015). Although not (and probably more correctly 'no longer') dust-rich, NGC 5813 is an old merger surrounded by a group-sized hot gas halo (Randall et al. 2015) that destroys dust, removes gas, and thereby inhibits star formation, preferentially impacting lower-mass galaxies. The second is NGC 7457 (dust=N, that is, a strong no) with cylindrical rotation about its major axis, revealing that it, too, experienced a merger, determined via other means to have occurred 2-3 Gyr ago (Sil'chenko et al. 2002; Chomiuk, Strader, & Brodie 2008; Hargis et al. 2011; Molaeinezhad et al. 2019). NGC 7457 displays an anti-truncated stellar disc and is somewhat unusual in that it is a merger that has lost its dust. However, this is plausible given its relatively low galaxy stellar mass of around 10^{10} M$_\odot$ compared to $\sim 10^{11}$ M$_\odot$ for the dust-rich merger-built S0 galaxies. Finally, two ES,b galaxies (NGC 5845 and NGC 1332, with dust=n, that is, only nuclear dust) are *suspected* major merger remnants given their embedded intermediate-scale discs, as noted in Section 3.3.

While the following S0 galaxies are not considered to have been built by a major merger and are not dust-rich, they have, however, experienced a minor merger or accretion event, leaving them still largely 'primaeval' in the sense of their stellar mass and structure, having not morphed into an S galaxy (Julian & Toomre 1966; D'Onghia, Vogelsberger, & Hernquist 2013; Graham 2023b). They are NGC 2787, NGC 3998, and NGC 4026 (all three categorised as dust=y), and NGC 1023, NGC 4762, and NGC 7332 (all three with dust=N). References to works discussing the merger history of these galaxies are provided in (Graham 2023a, Table 2).

For those thinking there is a lot to keep up with, we do not disagree. The notion that S0 galaxies are only faded or merged S galaxies (e.g. see the discussion of the colour-mass diagram by Schawinski et al. 2014) has been supplanted with the recognition of an additional primaevel S0 population from which the S galaxies formed. The high $M_{bh}/M_{\star,sph}$ ratios of these initial S0 galaxies, and their location in the $M_{bh}-M_\star$ diagrams, is what ruled out the previous two (faded or merged S galaxy) formation channels for this population of S0 galaxies. This revelation has also resulted in re-drawing the evolutionary paths in the colour-mass diagram (Graham 2024a). How the LRDs relate with this explicitly identified primaeval population is explored, for the first time, in this work.

2.1.2. UCD galaxies and NSCs

A local sample of UCD galaxies and NSCs with directly measured SMBH masses has come from Graham & Spitler (2009) and (Graham 2020, and references therein).[j] This sample includes the SMBH and NSC masses for the (stellar-stripped S0 and now) compact elliptical (cE) galaxy M32 (Nguyen et al. 2018) and the flattened 'peculiar'[k] dwarf ETG NGC 205 (Nguyen et al. 2019), plus an updated black hole mass for NGC 404 (Davis et al. 2020)[l] and NGC 4395 (Brum et al. 2019).[m] The sample is supplemented with the NSCs in NGC 5102, NGC 5206 (Nguyen et al. 2018; Nguyen et al. 2019)[n] and NGC 3593 (Nguyen et al. 2022). UCD736 orbiting within the Virgo Galaxy Cluster (Liu et al. 2020; Taylor et al. 2025) has also been added, as have the globular clusters B023-G078 around M31 (Pechetti et al. 2022) and ω Centauri (D'Souza & Rix 2013; Häberle et al. 2024) for which the *Gaia*-Sausage/Enceladus host galaxy mass is used (Lane, Bovy, & Mackereth 2023), as discussed by Limberg (2024). Finally, the dwarf spheroidal galaxy Leo I (Mateo, Olszewski, & Walker 2008) has been included, although it may not contain a massive black hole (Pascale et al. 2024).

The original $M_{bh}-M_{\star,nsc}$ relation, involving nuclear star cluster masses, $M_{\star,nsc}$, was first published in Graham (2016), having been presented at a 2014 IAU conference in Beijing. The relation was updated by (Graham 2020, Equation 6) and is shown in figure 1, along with the galaxy-morphology-specific $M_{bh}-M_{\star,sph}$ relations. The former relation stems from the discovery of the $M_{\star,nsc}-M_{\star,sph}$ relation (Balcells et al. 2003; Graham & Guzmán 2003) coupled with the $M_{bh}-M_{\star,sph}$ relation. It is important to recognise that it appears to hold until (i) the erosion of the star clusters at high black hole masses due to binary SMBHs (Bekki & Graham 2010; Gualandris & Merritt 2012) or (ii) the appearance of a nuclear disc 10s-to-100s of parsec in size rather than just an ellipsoidal star cluster. To date, the $M_{bh}-M_{\star,nsc}$ relation has not received anywhere near the attention of the $M_{bh}-M_{\star,sph}$ relation, yet it holds insight into the coevolution of dense star clusters and massive black holes with important consequences for gravitational wave science from

---

[g]Given their coincident location in the $M_{bh}-M_{\star,sph}$ diagram with S galaxies, a small handful of dust-poor S0 galaxies in the sample may be the gas-stripped and faded S galaxies proposed by Gunn & Gott (1972) and Davies & Lewis (1973).

[h]The four dust 'bins' (Y, y, n, N) were introduced and are described in Graham (2023a).

[i]The potentially depleted stellar core in NGC 5813 (Richings et al. 2011; Dullo & Graham 2014) is thought to be formed from the merger of a binary black hole (Begelman et al. 1980; Graham 2004). However, it may be worth remodelling this galaxy with an anti-truncated disc to check if the simpler Sérsic bulge model will suffice once this is implemented.

[j]The inner stellar component of M59-UCD3 may be a nuclear disc rather than an NSC.

[k]NGC 205 has dust patches and young stars near its centre (Haas 1998; Marleau et al. 2006).

[l]This mass is questionable as estimates from reverberation mappings suggest a black hole mass that is an order of magnitude smaller (Gu et al. 2024; Pandey et al. 2024).

[m]The nuclear star cluster mass is taken from den Brok et al. (2015).

[n]NGC 5102 and NGC 5206 would benefit from a bulge/disc decomposition rather than the single Sérsic model that has been fit to the main galaxy. The nuclear star cluster, rather than the nuclear star cluster plus nuclear disc, is shown here. As shown in Balcells et al. (2007), both nuclear components are common in S0 galaxies (e.g. Lyubenova et al. 2013).
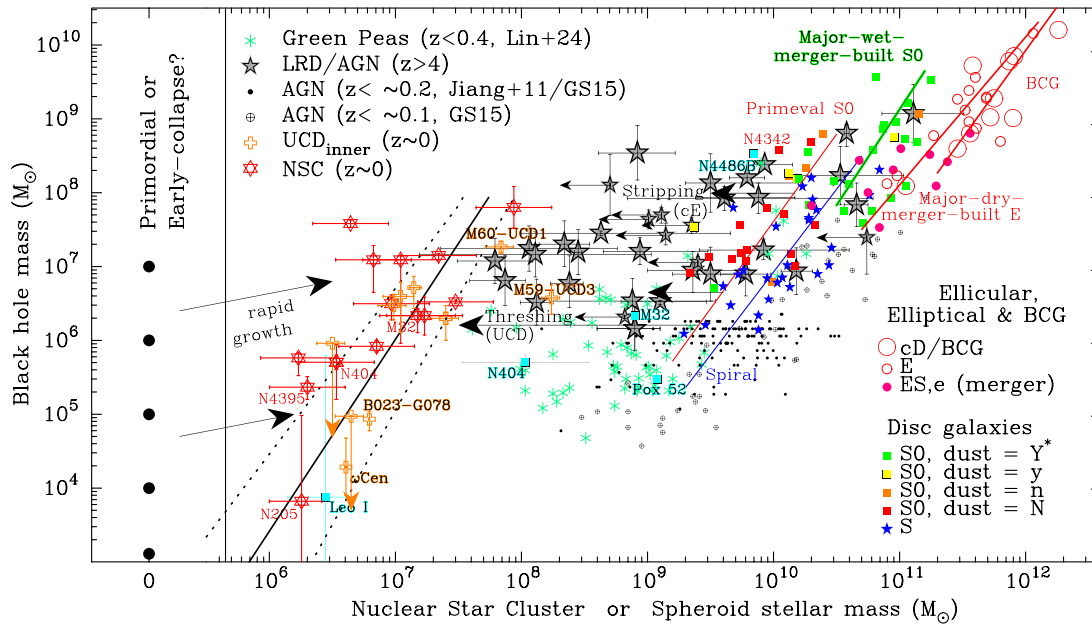
Figure 1. M_{bh}-$M_{\star,sph}$ diagram and relations. This is an extension of Figure 5 from Graham (2024b), itself an adaption of Figure 6 from Graham & Sahu (2023b). From right to left, the lines from existing studies are as follows. The right-most red line represents BCGs, and the second-from-right red line represents non-BCG E galaxies (Graham 2024b, Table 2), both primarily built from 'dry' major mergers. The green line represents ('wet' major merger)-built dust-rich (dust=Y) S0 *and* the Es,b galaxies (Graham 2024b, Table 2), hence the asterisk on the Y in the figure legend. Next, the blue line represents S galaxies (Graham 2023b, Table 1), while the orange line represents dust-poor (dust=N) S0 galaxies referred to here as primaeval (Graham 2023b, Table 1). Stripping and threshing the stars from these galaxies may produce cE and UCD galaxies, respectively. The left-most solid and dotted lines represent the NSCs and inner component of UCD galaxies (Graham 2020, Equation 6). Notes: Spheroid masses of AGN with $4 \times 10^6 \lesssim M_{bh}/M_\odot \lesssim 5 \times 10^7$ have likely been overestimated (in these suspected S galaxies, based on their location in figure 2). Without any structural decomposition of the LRDs, their total stellar mass is shown here under the implicit assumption, which we denounce (Section 3.2), that they are spheroidal structures without a disc component. Upper-left legend: Lin+24 = Lin et al. (2024b); 'LRD/AGN' covers the LRDs reported in recent works, as noted in Section 2; Jiang+11 = Jiang et al. (2011); GS15 = Graham & Scott (2015). The NSC and UCD data come from (Graham 2020, and references therein). Lower-right legend: Galaxies with directly measured SMBH masses (Graham & Sahu 2023a), with updates noted in Section 2. Cyan squares (and the green peas and grey AGN samples) are additional galaxies not used to derive the relations.

extreme mass ratio inspiral (EMRI) events (e.g. Preto & Amaro-Seoane 2010; Mapelli et al. 2012; Babak et al. 2017; Gair et al. 2017; Amaro-Seoane et al. 2023).

For the M_{bh}−$M_{\star,sph}$ diagram shown in figure 1, the stellar mass of the inner component of the UCD galaxies, i.e. the dense NSC obtained from decompositions of their light profiles, is displayed. For the M_{bh}−$M_{\star,gal}$ diagram (Figures 2 and 3), the total stellar mass of the UCD galaxies is presented. This latter approach mirrors the plotting of the total stellar mass for the 'ordinary' galaxies shown in figures 2 and 3, while their bulge or equivalently spheroid stellar mass is displayed in figure 1.

2.2. AGN with derived black hole masses

2.2.1. Low-z AGN

Estimated black hole masses from the compilation of low-redshift ($z \lesssim 0.2$) AGN used by Graham & Scott (2015) are presented in figures 1 and 2. The black hole mass estimates for the ten AGN from Reines et al. (2013) are reduced here by 0.75 to bring the virial factor used by Reines et al. (2013) in line with Graham et al. (2011). The compilation also includes eleven AGN from Busch et al. (2014), ten AGN from Mathur et al. (2012), two from Yuan et al. (2014), and UM 625 from Jiang et al. (2013). This sample is bolstered with a further 8 (=10-2)[o] confirmed AGN with 0.024 <

$z < 0.072$ from (Chilingarian et al. 2018, their Table 2). AGN data from Jiang et al. (2011), with $2 \times 10^5 \lesssim M_{bh}/M_\odot \lesssim 2 \times 10^6$, are also included, as is the cE galaxy SDSS J085431.18+173730.5 (Paudel et al. 2016) in figure 2.

There are 1-sigma uncertainties in individual AGN masses of a factor of 2 to 3 due to estimates based on Doppler-broadened Gaussian emission lines (Onken et al. 2004). The stellar mass-to-light (M/L) ratios are subject to systematic uncertainties related to the shape of the stellar initial mass function (IMF), internal dust attenuation, and mean stellar ages or star formation histories. The metallicity affects the amount of gas cooling (from emission lines) and in turn impacts the fragmentation of gas clouds into stars and, thus, the IMF.[p] Collectively, this can yield a factor of 2 uncertainty on the adopted stellar masses. Furthermore, the mass of the evolved stellar populations in today's galaxies may have been greater before the stellar-to-gas mass conversion arising from stellar winds and supernovae during the galaxy ageing process. Of course, some fraction of this second-generation gas may have turned into new stars. To avoid crowding, these uncertainties are not shown in the figures.

In passing, it is noted that Jiang et al. (2013) report that the galaxy UM 625 with an AGN can be convincingly categorised as hosting a pseudobulge due to its blue colour and Sérsic index $n < 2$. However, 'classical' bulges built from major wet mergers will

---

[o]J153425.58+040806.7 and J160531.84+174826.1 (from Chilingarian et al. 2018) are already included in the sample from Reines et al. (2013).

[p]In a relatively metal-poor early-Universe, the IMF is top-heavy, where as in today's relatively metal-rich environments, the IMF is bottom heavy.
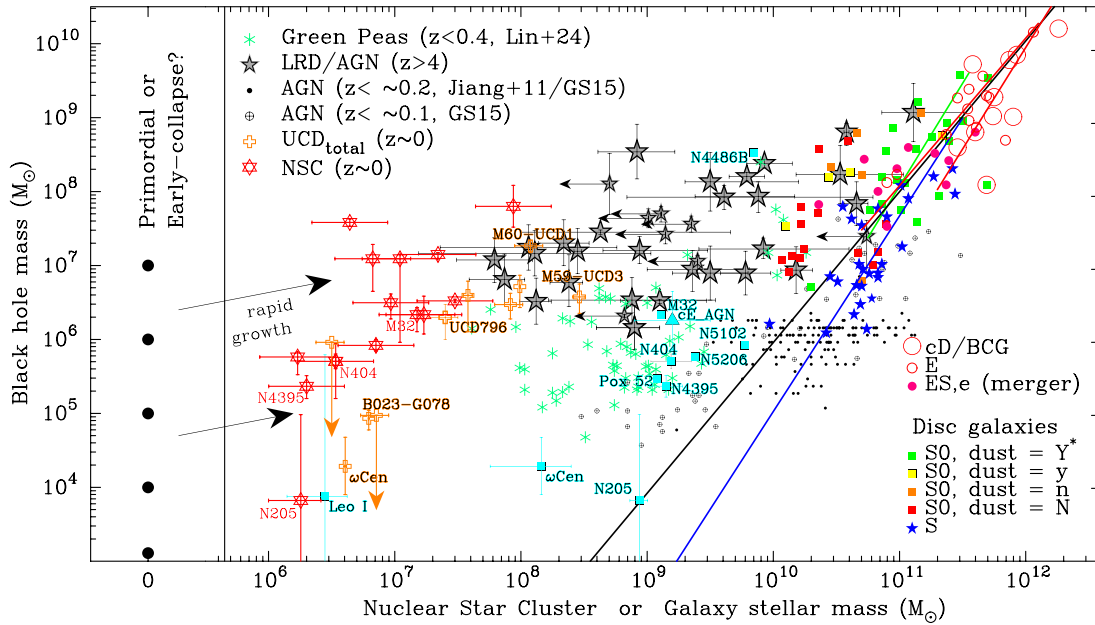
Figure 2. M_{bh}-$M_{\star,gal}$ diagram and relations. Modification of figure 1, building on Figure A4 from Graham (2023b). Here, the inner plus outer components of UCD galaxies are used for their galaxy stellar mass. The right-most red line (upper-right) denotes E BCGs, while the longer red line denotes non-BCG E galaxies (Graham 2024b, Table 2) and overlaps with the slightly steeper green line representing dust-rich (dust=Y) S0 and Es,b galaxies (Graham 2024b, Table 2). The long black line denotes galaxies built from major mergers (Graham 2023b, Table 1). The steepest (blue) line represents the S galaxies (Graham 2023b, Table 1), which follow a steep 'blue sequence' (Savorgnan et al. 2016; Davis et al. 2018). The very numerous (in the local Universe) dust-poor S0 galaxies (orange and red squares) with low stellar masses do not follow either of these relations. The LRD/AGN sample shown here comes from the 2023-2024 data sets mentioned in Section 2.2.2.
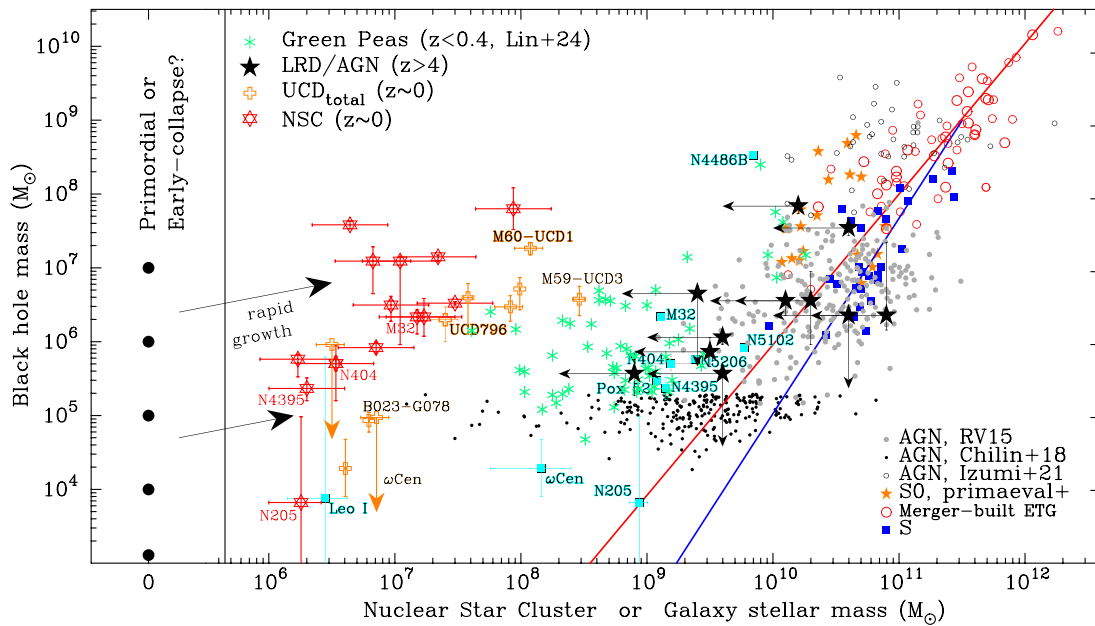
Figure 3. Modification of figure 2. The quasi-quadratic (black) line represents galaxies built from major mergers (Graham 2023b, Table 1) while the quasi-cubic (blue) line represents S galaxies (Graham 2023b, Table 1), known to follow the steeper 'blue sequence' discovered by Savorgnan et al. (2016). The $z < 0.055$ AGN (larger grey dots) from Reines & Volonteri (2015) have been added; they support the steep quadratic/cubic M_{bh}-$M_\star$ relations; that is, they are not an offset population. The smaller black dots are low-z galaxies with AGN hosting suspected intermediate-mass black holes (Chilingarian et al. 2018). The open black circles are $z \gtrsim 6$ AGN with dynamical, rather than stellar, galaxy masses (Izumi et al. 2021). Lower-right legend: RV15 = Reines & Volonteri (2015); Chilin'+18 = Chilingarian et al. (2018); Izumi+21 = Izumi et al. (2021); S = spiral galaxies with a directly-measured SMBH mass. 'Merger-built ETG' = S0, ES, E and BCG with a directly-measured SMBH mass and known to have been built from a major merger; 'S0, primaeval+' = dust-poor low-mass galaxies with a directly-measured SMBH mass and not known to have experienced a major merger; the + acknowledges that some of these overlap with the distribution of S galaxies and as such are likely to be faded S galaxies rather than faded/preserved S0 galaxies that never sufficiently grew to host a spiral pattern. The LRD/AGN sample shown here is from Rusakov et al. (2025) and has only upper limits for the stellar masses.

have lingering star formation (Graham, Jarrett, & Cluver 2024), and their bulges can have $n < 2$ (e.g. Sahu, Graham, & Davis 2020; Graham 2024b). Moreover, the high bulge-to-total (B/T) ratio of 0.6 reported by Jiang et al. (2013) additionally favours a merger origin. UM 625 likely represents an endemic misclassification of bulges, an issue raised by Graham (2014). This situation is reminiscent of that with other dust-rich S0 galaxies built from major wet mergers, such as NGC 1194, NGC 1316, NGC 5018 and NGC 5128, which reside below the old near-linear $M_{bh}-M_{\star,sph}$ relation for ETGs but on the steep $M_{bh}-M_{\star,sph}$ relation for merger-built (dust-rich) S0 galaxies (Graham 2023a).

It is additionally noted that *galaxy* stellar masses were used for some of the 34 AGN with $z \sim 0.1$ in the $M_{bh}-M_{\star,sph}$ diagram (Figure 1). Specifically, the galaxies from Yuan et al. (2014) and Reines et al. (2013) were, in the absence of bulge/disc decompositions, effectively taken to be E galaxies. If they are S or S0 galaxies, then the above practice will have acted to shift them rightward in figure 1. Such a shift also occurs when using bulge masses if the B/T ratios of the disc galaxies have been overestimated. This appears to be the situation with the AGN data from Busch et al. (2014) and Mathur et al. (2012) based on the agreement of their AGN sample with the inactive S galaxies in the $M_{bh}-M_{\star,gal}$ diagram (Figure 2).

A second $M_{bh}-M_{\star,gal}$ diagram (Figure 3) has been made with alternate sources of AGN data. This was done, in part, to avoid crowding. The other (main) reason was to provide a diagram that better distinguishes the primaeval S0, S, and merger-built galaxies with directly measured black hole masses. The estimated black hole masses in the AGN from Reines & Volonteri (2015) and the entire sample of 305 intermediate-mass black holes candidates with $4 \times 10^4 \lesssim M_{bh}/M_\odot \lesssim 2 \times 10^5$ from Chilingarian et al. (2018) are shown in figure 3.[q] The SMBH masses from Reines & Volonteri (2015) are reduced here by 0.7 (=0.75/1.075) to ensure a consistent virial factor, $f = 3$, with the above AGN samples. In addition, data from Lin et al. (2024b) for 59 'green peas'[r] with $z < 0.4$ are shown, as are the $z \gtrsim 6$ AGN data from Izumi et al. (2021), as noted in the following subsection.

2.2.2. High-z AGN and LRDs

Many teams have reported measurements of the stellar mass associated with high-z AGN. Before *JWST* data, Izumi et al. (2018) and Izumi et al. (2021) presented a compilation of AGN at $6 \lesssim z \lesssim 7$. They stressed how sample selection bias of bright QSOs at these high redshifts had swayed the conclusions from past investigations. Their compilation rectified this situation by including lower luminosity QSOs at the same high redshifts. Their data compilation is shown here in figure 3, although it is noted that the galaxy masses are dynamical rather than stellar, and, as such, smaller symbols have been used for this sample. Their SMBH masses were based on the prescriptions given by Vestergaard & Peterson (2006), calibrated to a virial factor $f = 5.5$ (Onken et al. 2004). Here, these SMBH masses have been reduced by a factor of 3/5.5, which is in agreement with the calibration used by Graham & Scott (2015).

JWST has enabled the detection of AGN in LRDs over a wide range of high redshifts ($\sim$3-4 to $\sim$9-11). Image resolution inhibits our ability to discern multiple components in these LRDs. LRD data from the studies listed below have been included in figures 1–2, with the *same* total stellar mass presented in both diagrams. The associated error bars are taken from the published works.

The high-z galaxy data shown here are from (Kokorev et al. 2023, one AGN at $z = 8.502$), (Furtak et al. 2024, one AGN at $z = 7.045$), (Larson et al. 2023, one AGN at $z = 8.679$), (Tripodi et al. 2024, one AGN at $z = 8.632$), (Maiolino et al. 2024, GNZ11 at $z = 10.603 =$ GNZ11), (Carnall et al. 2023, one AGN at $z = 4.658$), (Übler et al. 2023, one AGN at $z = 5.55$), (Juodžbalis et al. 2024, one dormant black hole at $z = 6.68$), (Ding et al. 2023, two AGN at $z = 6.34$ and 6.40), (Kocevski et al. 2023, two AGN at $z = 5.242$ and 5.624), (Wang et al. 2024, two AGN at $z = 6.68$ and 6.98)[s], (Harikane et al. 2023, 9 AGN at $4 < z < 6$ plus one at $z = 6.936$), and (Maiolino et al. 2024, 12 new AGN at $4 < z < 7$).

Uncertainties in the wavelength-dependent contributions of AGN and starlight to the spectral energy distribution (SED) can influence the H_α, H_β, and He I broad line equivalent width measurements and thus impact the AGN masses (e.g. Wang et al. 2024). Moreover, after submitting this paper, the published stellar and black hole masses of these high-z AGN continued to be debated as researchers probed the SED and the origin of the line broadening (Rusakov et al. 2025; de Graaff et al. 2025; Naidu et al. 2025). As with NGC 1068 (Miller, Goodrich, & Mathews 1991) and NGC 4395 (Laor 2006), Rusakov et al. (2025) report that the primary line-broadening mechanism in the distant AGN/LRDs appears to be electron scattering through a dense Compton-thick ionised gas (producing lines with exponential profiles) rather than Doppler motions (producing Gaussian or centrally broad profiles) that were found to play a lesser role. They show how this reduces the estimated black hole masses by 2 orders of magnitude, although it remains unclear what the revised stellar masses are, with Rusakov et al. (2025) only reporting massive upper limits. The actual stellar masses are expected to be smaller because not enough time has elapsed for such massive galaxies to arise. Their data is shown in figure 3. In passing, it is remarked that some of the high-z quasars and QSOs reported to have very large black holes over the past 10–20 yr will also have had their black hole masses overestimated *if* the broadening of their emission line(S) is mostly due to electron scattering. It may, therefore, be worthwhile reexamining the shape of the line profiles and checking for a broad plus narrow component in some of those systems.

3. Context setting and discussion of results

3.1. Background briefing

For those new to the evolving field of black hole scaling relations, a recap of select relevant developments over the past decade may be helpful. Other readers may wish to jump to Section 3.2.

As explained in Graham (2012), it is understood why a near-linear $M_{bh}-M_{\star,sph}$ relation is inadequate to describe 'ordinary' galaxies with 'classical' (merger built) bulges (as observed by Laor 1998; Laor 2001; Wandel 1999; Salucci et al. 2000). It is now recognised that each galaxy type follows a notably steeper than

---

[q]Aside from the ten (8 + 2) AGN from Chilingarian et al. (2018) that are mentioned above and shown in figure 2, just one other AGN (SDSS J122548.86+333248.7) from Graham & Scott (2015) appears in the larger sample from Chilingarian et al. (2018) presented in figure 3.

[r]'Green peas' are luminous but low-mass ($\lesssim 10^{10}$ $M_\odot$) compact galaxies with substantial star formation (Cardamone et al. 2009).

[s]We took the 'medium' stellar masses and associated AGN masses from Wang et al. (2024), noting the data in their Table 1 does not match that in their Figure 8.

linear distribution (Graham 2023b), and recognition of galaxy-morphology-specific relations has enabled considerable breakthroughs in our understanding of galaxy evolution. For example, recognition of the galaxy-morphology-dependent $M_{bh}-M_{\star,sph}$ relations has led to the identification of two types of S0 galaxies (those known to have low-metallicities and old ages are referred to as primaeval (Conselice, Gallagher, & Wyse 2003; Lisker et al. 2006; Sil'chenko 2013; the other is built from wet major mergers Graham 2023a). In the past, these primaeval galaxies may have accreted gas and experienced minor mergers in such a way that they morphed into S galaxies, or a substantial collision may have led them to bypass such a transition and become a second-generation major-merger-built S0 galaxy, which can also be made from S galaxy collisions. Graham (2023b) has suggested that these low-mass, dust-free S0 galaxies are preserved, albeit faded, primaeval galaxies. Ram-pressure stripping of cold gas from these galaxies within the hot X-ray emitting gas clouds/haloes of galaxy groups and clusters can act to preserve them by shutting down star formation. The high velocities of the galaxies in the clusters inhibit mergers of the low-mass galaxies and prevent this avenue of evolution. The cluster environment effectively 'pickles' these galaxies.[t] The bulk of this galaxy type, often referred to as dwarf ETG (dETG), are known to be nucleated (e.g. Binggeli et al. 1985; Sandage, Binggeli, & Tammann 1985), with even more found using the *Hubble Space Telescope* (e.g. Lotz et al. 2001; Graham & Guzmán 2003; Côté et al. 2006). As galaxy mass functions show, they, and dwarf irregular galaxies, are the most abundant galaxy type in the Universe today (e.g. Reaves 1983; Phillipps et al. 1987). If they contain massive black holes, mergers of these systems, likely in the pre-cluster field and group environment, erode the central star cluster and thereby reduce the central surface brightness (Bekki & Graham 2010).

As early as Romanishin et al. (1977), some of these dETGs were considered dS0 disc galaxies. This has contributed to replacing the Tuning Fork diagram with an evolutionary scheme, dubbed the 'Triangal', linking the galaxy types through accretions and mergers (Graham 2023b). It is the objective of this manuscript to begin to place LRDs in this greater context of galaxy evolution. The impact of mergers is widespread and wide-scale, from the erosion of NSCs to a potential 'merger bias'[u] affecting measurements of the baryonic acoustic oscillations (BAO) used to probe cosmology (Eisenstein et al. 2005; Percival et al. 2007).[v] As we shall see in Section 3.3, these morphology-specific relations are also important for understanding the distribution of AGN in the $M_{bh}-M_{\star}$ diagram. The distribution of the $z = 0$ primaeval S0 galaxies is additionally important for checking potential connections with the distant AGN/LRDs, as done in Section 3.2.

Finally, it may be helpful to note that a detected offset in an $M_{\star}$-σ diagram between ETGs with and without directly measured

black hole masses, which had potentially implied a bias in the $M_{bh}-M_{\star}$ relations derived from galaxies with directly measured black hole masses (Shankar et al. 2016), was entirely due to a mismatch in the stellar light-to-mass conversion between the data sets (Sahu, Graham, & Hon 2023). The $M_{bh}-M_{\star}$ relations should be applied as is to galaxies without directly-measured black hole masses; one simply needs to ensure that the stellar masses of one's sample are derived consistently with that used to establish the scaling relation.[w]

3.1.1. Compact massive red nuggets

Although not highlighted in the figures, we mention the local massive 'compact galaxies' (Zwicky & Kowal 1968; Zwicky & Zwicky 1971) given that some works (e.g. Trujillo et al. 2014; Saulder, van den Bosch, & Mieske 2015) are renaming these 'relic galaxies' due to their similarity to the compact massive galaxies at $z \sim 2.5 \pm 1$, aka 'red nuggets' (Daddi et al. 2005; van Dokkum et al. 2008; Damjanov et al. 2011). They have sizes and masses comparable to the bulges of today's merger-built dust-rich S0 galaxies (Graham 2013; Hon, Graham, & Sahu 2023) and encapsulate the ES,b galaxies shown in Graham & Sahu (2023b). Some red nuggets were found at $z < 0.6$ using *SDSS* data (Damjanov et al. 2014), with one of the objects being an extremely compact post-starburst galaxy at $z = 0.5$. Here, the four ES,b galaxies (with *Spitzer Space Telescope* imaging and multicomponent decompositions) have been grouped with the dust-rich S0 galaxies.

For readers unfamiliar with the ES galaxy type introduced by (Martha) Liller (1966), they have embedded, intermediate-scale stellar discs that do not dominate the light at large radii (e.g. Nieto, Capaccioli, & Held 1988; Arnold et al. 2011; Graham et al. 2012; Buta et al. 2015; Savorgnan & Graham 2016b).[x] As noted in the Introduction of Graham (2024b), this population is similar, but not equal, to the 'discy ellipticals' presented by Nieto et al. (1988), Nieto & Bender (1989), and Scorza & Bender (1995). The ES,b galaxies are compact and akin to bulges, while the ES,e subtype are extended and more like E galaxies (Graham & Sahu 2023b). Residing near the top of the wet-major-merger-built S0 galaxy sequence, the ES,b galaxies may be relic mergers. This would then rule them out as larger evolved counterparts of LRDs in the sense of evolution by simple gas accretion. Red nuggets might, however, be morphed descendants of LRDs in the sense of a (major merger)-induced 'punctuated equilibrium' event, i.e. collision, that transformed the primaeval discs into these more bulge-dominated galaxies at high redshift.

Although multiple stellar populations were not detected in the local ES,b galaxies Mrk 1216, NGC 1271, or NGC 1277 (Walsh et al. 2015; Y ld r m et al. 2015) – which might be odd given their bulge/disc nature if not for their old ages – Rusli et al. (2011) tentatively report different populations in NGC 1332 (dust=y) and Poci et al. (2019) measure differences within NGC 3115 (dust=Y), which is reported to have a spatially offset AGN due to a past merger (Menezes, Steiner, & Ricci 2014). The ES,b galaxy NGC 1277 became well known after it was thought to have an over-massive black hole giving an $M_{bh}/M_{\star,sph}$ ratio of

[t]Some distant LRDs have been observed in overdense regions (e.g. Larson et al. 2022; Schindler et al. 2024; Mérida et al. 2025).

[u]'Merger bias' is a term introduced here to capture how luminous red galaxies (LRGs) merge and thus reduce in number over time when building BCGs in clusters that trace the BAO boundary walls. At the same time, new LRGs, such as dust-rich S0 galaxies, form from lower-mass mergers in groups (with lower velocity dispersions congenial to mergers) that are initially out of clusters but fall towards them over time (Sawangwit et al. 2011; Angulo et al. 2014; Kim et al. 2015). Such spatial evolution in the distribution of LRGs due to mergers might introduce an evolving bias with redshift that skews BAO 'standard ruler' measurements, complicating claims about an evolving dark energy equation of state.

[v]The abundance of AGN with redshift offers another probe of the time evolution of the equation of state parameter (Lamastra et al. 2012).

[w]The $M_{bh}-M_{\star}$ relations for the galaxies shown here were obtained using a diet-Salpeter IMF (Bell & de Jong 2001). Conversion factors for other IMFs are available in Graham & Sahu (2024).

[x]Buta et al. (2015) labelled many ES galaxies S0$^-$ sp/E5-E7. However, the (E1-E4)-looking galaxies can also be ES galaxies with either face-on or edge-on discs at interior radii.

0.59 (van den Bosch et al. 2012). However, the black hole mass was overestimated by an order of magnitude and the spheroid mass underestimated by the same amount (Graham et al. 2016a). As such, NGC 1277 is not considered an analogue of an LRD with a particularly high $M_{\rm bh}/M_{\star,\rm sph}$ ratio. The large, extended ES,e galaxies highlighted in the figures have similar B/T ratios to the ES,b galaxies. They are built by (perhaps lower redshift) mergers (Graham 2024b, and references therein). However, they have notably lower $M_{\rm bh}/M_{\star,\rm sph}$ ratios and lower stellar densities within their spheroid's half-light radii (Graham & Sahu 2023b, their Table 1).

3.2. *LRDs with AGN*

Figure 1 shows that NSCs and the dense inner components of UCD galaxies have stellar masses 2–3 orders of magnitude smaller than local galaxies with the same black hole mass. Curiously, they roughly follow a distribution with a similar slope in the $M_{\rm bh}$-$M_{\star,\rm sph}$ diagram. Although new NSC and UCD galaxy data have been included (see Section 2.1.2), the line shown on the left-hand side of figure 1 has been taken from Graham (2020) and is essentially that first reported by Graham (2016). In a future paper, an updated analysis of this relation will be presented. The main objective here is to see how the LRDs compare. In figures 2–3, the total (NSC + envelope) stellar mass of the UCD galaxies is displayed.

Many ideas exist as to how SMBHs established themselves early in the Universe (e.g. Inayoshi, Visbal, & Haiman 2020, and references therein). At first glance, the high (2023–2024 and 2025) SMBH masses reported for the LRDs/AGN at high-z may seem to favour heavy black hole seeds over light seeds, and one might even speculate that they could be primordial, contributing to dark matter (e.g. Argyres, Dimopoulos, & March-Russell 1998; Bean & Magueijo 2002; Dolgov & Postnov 2017). The direct collapse of gas clouds (Doroshkevich, Zel'dovich, & Novikov 1967; Umemura et al. 1993) and self-gravitating pre-galactic gas disks (Begelman et al. 2006; Spaans & Silk 2006) has been proposed for the production of the more massive seed black holes. At the same time, there can still be a contribution from light black hole seeds, including those built from the cascading collision of stars in dense clusters at the nuclei of haloes (Portegies Zwart & McMillan 2002; Omukai, Schneider, & Haiman 2008; Das et al. 2021). In the presence of substantial gas, dynamical friction will help feed these cluster stars inward (Omukai et al. 2008; Devecchi & Volonteri 2009; Davies, Miller, & Bellovary 2011). This will contribute to the partial demise of the clusters and the growth of the massive black holes. There is also near-Eddington (Wolf et al. 2024) and super-Eddington accretion (Volonteri & Rees 2005; Alexander & Natarajan 2014) onto these high-z black holes, perhaps formed from Pop III stars (Ryu et al. 2016; Banik et al. 2019; Tan et al. 2024). Indeed, Suh et al. 2025) recently reported on LID-568, an SMBH at $z \approx 4$, accreting at 40 times the Eddington limit. A combination of light and heavy black holes may have seeded the LRDs.

There may be clues at low-z as to the evolution of LRDs. The cE galaxies at $z \sim 0$ are considered former low-mass ETGs stripped of many of their stars (e.g. Zinnecker et al. 1988; Freeman 1993; Khoperskov et al. 2023). At the same time, some rare isolated cEs may have simply never 'grown up', unless they are all runaway systems that were stripped and then ejected from galaxy groups or clusters (Chilingarian & Zolotukhin 2015). As illustrated in (Graham & Sahu 2023b, their Figure 6), stripping

of stars can produce galaxies with $M_{\rm bh}/M_{\star,\rm sph} \approx 0.05$ (e.g. NGC 4486B around M87, or NGC 4342). The more extreme version of stripping, referred to as 'threshing' (e.g. Bekki & Freeman 2003; Ideta & Makino 2004; Chilingarian & Mamon 2008; Pfeffer & Baumgardt 2013), is thought to produce UCD galaxies. SDSS J124155.33+114003.7 (M59cO) may represent a halfway point between cE and UCD galaxies (Chilingarian & Mamon 2008). Threshing can pare a galaxy back to $M_{\rm bh}/M_{\star,\rm sph} \sim 0.1$ (e.g. UCD1 around M60) or perhaps even ~ 1 if just the NSC remains.

Given that the stripping process should preferentially remove the dark matter (thought to be dominant at larger, and thus less bound, radii),[y] a key difference between local UCD galaxies formed via stripping and relic LRDs may be their dark matter fraction. The lack of dark matter in UCD galaxies (e.g. Hilker et al. 2007; Chilingarian, Cayatte, & Bergond 2008; Chilingarian et al. 2011; Frank et al. 2011) would seems to rule out the notion they are relic compact galaxies formed long ago in dark matter haloes, i.e. relic LRDs, as opposed to tidally-stripped galaxies. Furthermore, the *first* LRDs to form are perhaps unlikely to be today's UCD galaxies, as these early LRDs probably resided in larger over-densities that eventually became today's massive ETGs. However, the LRDs that formed later in the Universe, in smaller haloes, might be the ancestors of today's UCD galaxies, that is, they could be the nuclei of threshed low-mass disc galaxies that started life as LRDs. One may also speculate that all of today's UCD galaxies should contain a massive black hole *if* all high-z LRDs did. It is not, however, established that all local UCD galaxies contain a massive black hole, nor if all nucleated dwarf ETGs galaxies – the likely pre-stripped progenitors of UCD galaxies – do. This state of affairs is an issue of spatial resolution and, therefore, probably does not yet provide useful constraints.

Based on the 2023–2024 masses for LRDs, they are not similar to NSCs for which Graham & Spitler (2009) quantified their $M_{\rm bh}/M_{\star}$ ratios. Figure 2 reveals that the LRDs tend to have smaller $M_{\rm bh}/M_{\star}$ ratios, with some matching that of UCD galaxies.[z] Through the LRDs, we may be witnessing the reverse of a stellar stripping process, in which the black hole mass is already in place or quickly forms before the bulk of a galaxy's stellar mass builds around it (e.g. Kokorev et al. 2024b, their section 5.2) and (Tripodi et al. 2024). However, with the revised black hole masses in the distant AGN/LRDs studied by Rusakov et al. (2025), figure 3 reveals that they require more definitive stellar masses before firm conclusions can be reached. It is considered unlikely that the LRDs evolve along the steep $M_{\rm bh}$-$M_{\star,\rm gal}$ relations defined by local galaxies because if their current upper stellar mass estimates (shown in figure 3) are close to their true stellar masses, then their small half-light sizes (tens to a few hundred parsec) would imply a problematically high stellar density. LRDs likely have considerably lower stellar masses than the upper limits shown in figure 3, perhaps overlapping with the green peas or perhaps forming an extension towards the UCD galaxies and NSCs in the $M_{\rm bh}$-$M_{\star,\rm gal}$ diagram.

Finally, we are open to the possibility that whether UCD galaxies and some LRDs are structurally equivalent could be a case

---

[y]Proponents of modified gravity offer an alternate view (Milgrom 1983; Moffat 2006; De Felice & Tsujikawa 2010; Famaey & McGaugh 2012; de Martino et al. 2020, their Section 5.1).

[z]The LRD with the exceptionally high mass is SDSS J2236+0032 (Ding et al. 2023). In Figure 2, it resides next to the ES,b galaxy NGC 1332 and the dust-rich S0 galaxy NGC 6861, suggesting it is more akin to a 'red nugget' than an LRD, as does its half-light radius of 0.7±0.1 kpc in the F356W filter (Ding et al. 2023).

of 'nave realism' based on 'the illusion of information adequacy' (Gehlbach, Robinson, & Fletcher 2024), stemming from their congruent location in the M_{bh}–$M_{\star,gal}$ diagram. Additional information may suggest that their overlap in SMBH and stellar masses is a mere coincidence. In this regard, size information of LRDs and age estimation of UCD galaxies (e.g. Chilingarian et al. 2008) should be valuable. At least some UCD galaxies are measured to be reasonably old, such as the Sombrero galaxy's SUCD1 at 12.6±0.9 Gyr (Hau et al. 2009) and M60-UCD1 with a formal age of 14.5±0.5 Gyr (Seth et al. 2014), older than the Universe. However, the Virgo cluster's VUCD3 is reported to have an age of just 11 Gyr with a 9.6-Gyr-old inner component, while M59cO has an age of 11.5 Gyr but with a blue inner component (Chilingarian & Mamon 2008) dated at just 5.5 Gyr old (Ahn et al. 2017). This may reflect the ability of star clusters to rejuvenate themselves, at least those residing at the bottom of a galaxy's gravitational potential well, or a late-time creation for some. Detecting *elongated* LRD host galaxies with light profiles having Sérsic indices $n \lesssim 1$ would suggest they are disc-like structures, whereas a distribution of somewhat spherical shapes would match that of local dETGs (e.g. Binggeli & Popescu 1995). While single Sérsic fits to galaxies with point-like AGN may yield small sizes, when the imaging data permits it, simultaneously fitting a point-source plus a Sérsic model may enable more reliable information on the underlying host galaxy.

In passing, it is noted that the stellar population of LRDs (and red nuggets) would have initially been blue due to hot, massive stars, just as the stars in the discs of today's low-mass disc-dominated S0 galaxies would have been more[aa] blue in the past when they were younger. Ideally, future work will reveal further connections between LRDs and 'green peas' (Cardamone et al. 2009; Lin et al. 2025), blue dwarf ETGs (Cairós et al. 2001, 2003; Driver et al. 2007; Cameron et al. 2009; Moffett et al. 2019), and luminous blue compact galaxies (Guzmán et al. 2003; Shi et al. 2005; Bergvall et al. 2006; Pérez-Gallego et al. 2011).

3.3. Additional AGN: Toeing the line

As noted in the Introduction, the steep quadratic nature of the M_{bh}–$M_{\star,sph}$ relations for ETGs built from major mergers naturally place bright QSOs (e.g. Wang et al. 2010; Bongiorno et al. 2014; Wang et al. 2016; Shao et al. 2017; Decarli et al. 2018; Venemans et al. 2016) above the original near-linear relation. At the same time, the super-quadratic M_{bh}–$M_{\star,sph}$ (and cubic M_{bh}–$M_{\star,gal}$) relation for S galaxies naturally places faint Seyfert galaxies below the original near-linear relation. Bridging these extremes are the low-luminosity QSOs and regular AGN of intermediate-luminosity (Willott, Bergeron, & Omont 2015; Willott, Bergeron, & Omont 2017; Izumi et al. 2018) that overlap with the original near-linear M_{bh}–$M_{\star}$ relation. Izumi et al. (2021) reported how the less luminous QSOs beyond $z \sim 6$ had $M_{bh}/M_{\star}$ ratios more in line with the original near-linear M_{bh}–$M_{\star}$ relation. Rather than talking in terms of differing and disjoint populations of AGN with over- or under-massive black holes, it makes more sense to recognise that the original proposition of a linear M_{bh}–$M_{\star}$ scaling relation requires adjusting and that a steeper scaling relation unifies many galaxies.

Unfortunately, the lack of morphological information among AGN samples has hampered past understanding of galaxy speciation. However, as briefly noted before, one slight mystery has now been resolved. In figure 1, and the M_{bh}–$M_{\star,sph}$ diagram presented in Graham & Scott (2015), some of the AGN were seen to reside to the right of the sample of galaxies with predominantly inactive black holes with directly measured masses. This is evident at $M_{bh} \approx 10^7$ M$_\odot$. From the M_{bh}–$M_{\star,gal}$ diagram (Figure 2), it is apparent that these AGN are probably S galaxies. It is likely that the published B/T ratios for these AGN, which were typically greater than 0.5-0.6, were too high, thereby artificially shifting them to the right in the M_{bh}–$M_{\star,sph}$ diagram. S galaxies tend to have $B/T < 0.1$–0.2 (Graham & Worley 2008; Davis et al. 2019).

Given the location of the AGN with $M_{bh} \lesssim 10^6$ M$_\odot$ in figures 1 and 2, they appear to be hosted by S galaxies and primaeval S0 galaxies. Again, the term primaeval is used to imply a first-generation galaxy type not altered by substantial accretion or major mergers. These AGN are consistent with the steep morphology-specific M_{bh}–$M_{\star}$ scaling relations, even though they were not used to define them.

A simplified variant of figure 2 is presented in figure 3, such that the local sample of galaxies with directly measured SMBH masses is now separated into just three types. There are those previously identified as primaeval; they are the low-mass, dust-poor S0 disc galaxies that tend to have an old, metal-poor stellar population. Second are the disc galaxies with a spiral pattern, which tend to have ongoing star formation.[ab] Then there are the galaxies built from major mergers, such as the (often dust-rich) S0 galaxies built from a wet major merger, the E galaxies built from a dry major merger, and the BCG typically built from more than one major merger. This subdivision offers an alternative view of how the local AGN mesh with, rather than deviate from, galaxies with varying formation histories.

Figure 3 also displays new samples of AGN. The AGN with estimated black hole masses from Reines & Volonteri (2015) and Chilingarian et al. (2018) are included, as are the AGN at $z \gtrsim 6$ from Izumi et al. (2021). However, only dynamical, rather than stellar, galaxy masses are published for this final sample. Therefore, a (not overly prominent) small circle is used to show those systems in figure 3. While (Izumi et al. 2021, their Figure 13) reported that many of these systems have 'overmassive' black holes (by up to a factor of ∼10) relative to the old near-linear M_{bh}-$M_{\star}$ relation, the bulk of them are not outliers relative to the steeper galaxy-morphology-dependent M_{bh}-$M_{\star}$ relation for merger-built S0 galaxies, a point made by Graham (2023a), see also Graham & Sahu (2023a). Just 3–5 of these AGN from Izumi et al. (2021) have M_{bh}/M_{dyn} ratios that are a factor of (only) 2–3 times higher than the distribution seen for local systems with directly measured SMBH masses. This is reconcilable with the sample selection bias of the most luminous QSOs at high-z and the greater inaccuracy of indirect measures of black hole mass in AGN. The subset of luminous $z \gtrsim 6$ AGN from Izumi et al. (2021) shown in figure 3 is likely to be wet-merger-built S0 galaxies.

At $M_{\star,gal} > 10^{10}$ M$_\odot$, in figure 3, the overlap of low-z AGN with the $z \approx 0$ sample of SMBHs with directly measured masses reveals that these AGN are predominantly S galaxies or merger-built S0 galaxies. These AGN are not an offset population from ordinary galaxies with predominantly inactive SMBHs. This information

---

[aa] Due to low metallicity, dwarf S0 galaxies are at the blue/green end of the 'red sequence' (Baum 1959; de Vaucouleurs 1961; de Vaucouleurs & de Vaucouleurs 1972; Graham 2024a, and references therein).

[ab] Arguably, gas-stripped and faded S galaxies, which are now S0 galaxies, belong to this category.

is crucial if we are to connect the evolutionary path of high-*z* AGN/LRDs with other active and inactive galaxies.

Knowledge of galaxy-morphology-specific black hole scaling relations enables an improved means for deriving the virial factor(s) for converting AGN virial products into black hole masses (Peterson 1993; Onken et al. 2004; Bentz et al. 2009). To date, these conversion factors have been obtained with little attention to galaxy morphology. A better approach will involve matching AGN virial products with directly measured black hole masses from galaxies *of the same morphological type* (Graham et al. 2025, in preparation). It can already be seen in the data of (Bentz & Manne-Nicholas 2018, their Figure 5) that the reverberation-mapped AGN follow a steep $M_{\rm bh}-M_{\star,\rm sph}$ distribution well-matched by the super-quadratic relation quantified by (Scott et al. 2013, their Figure 3) for galaxies without depleted stellar cores, i.e. those not built from a dry major merger. Similarly, the AGN data of (Bentz & Manne-Nicholas 2018, their Figure 6) display a steep trend similar to that of Savorgnan et al. (2016) for S galaxies. This yet-to-be-applied approach at determining the virial factor(s) will avoid a bias such that the reverberation-mapped AGN sample may be skewed towards a distribution of galaxy type, such as S and dust-rich S0 galaxies, that differs from the bulk of the sample with directly measured black hole masses to which it is compared. Similarly, AGN sample selection of certain galaxy types and not others, for example, S and/or dust-rich S0 but not primaeval dust-poor S0 galaxies or 'red and dead' E galaxies, may also explain the tight AGN relations reported by Bennert et al. (2021). The location of the LRDs and other AGN in figures 1–3 can be refined once improved virial factors, used to calibrate secondary relations, are established through application of the galaxy-morphology-dependent scaling relations (Graham 2023b). Better constraints on the stellar masses of the LRDs are also needed to decipher their evolutionary trajectory in the $M_{\rm bh}$-$M_\star$ diagrams.

4. Summary

This paper added high-*z* AGN/LRDs and low-*z* AGN to $M_{\rm bh}$-$M_\star$ diagrams that, for the first time, included local compact stellar systems (UCD galaxies and NSCs) in addition to larger galaxies with directly measured black hole masses. Our diagrams also included an expanded recognition of local galaxy morphologies and galaxy-morphology-specific $M_{\rm bh}$-$M_\star$ relations rather than a single near-linear relation for low-*z* galaxies with AGN and a separate single near-linear relation for $z \approx 0$ inactive galaxies. Unlike previous $M_{\rm bh}$-$M_\star$ relations based on various fractions of ETGs and LTGs, or all of the different ETGs combined, these morphology-specific relations avoid sample selection bias from mixing different galaxy types that follow distinct $M_{\rm bh}$-$M_\star$ relations.

The 2023–2024 LRD data are seen to span the $M_{\rm bh}$-$M_{\star,\rm gal}$ diagram from UCD galaxies to previously recognised primaeval S0 galaxies. With only upper limits on the recent 2025 stellar masses of LRDs (Rusakov et al. 2025), they remain consistent with local NSCs and UCD galaxies, low-*z* green peas, and primaeval local S0 galaxies. An improved knowledge of the LRD stellar masses is needed.

We demonstrated that several samples of low-*z* AGN, including candidate intermediate-mass black holes (Graham & Scott 2015; Chilingarian et al. 2018), broadly overlap with the steep, non-linear, galaxy-morphology-dependent $M_{\rm bh}$-$M_\star$ relations defined by predominantly inactive galaxies. This suggests that using galaxy samples with similar morphology should be worthwhile for re-determining the virial factor used to estimate

black hole masses in LRDs and AGN more broadly. Adjustments to high *z* QSO and LRD black hole masses will impact expectations for black hole seed masses, early accretion rates, and connecting the past with today.

References

Ahn, C. P., et al. 2017, ApJ, 839, 72

Akins, H. B., et al. 2024, arXiv e-prints, p. arXiv:2406.10341

Alexander, T., & Natarajan, P. 2014, Sci, 345, 1330

Amaro-Seoane, P., et al. 2023, LRR, 26, 2

Angulo, R. E., White, S. D. M., Springel, V., & Henriques, B. 2014, MNRAS, 442, 2131

Argyres, P. C., Dimopoulos, S., & March-Russell, J. 1998, PhLB, 441, 96

Arnold, J. A., Romanowsky, A. J., Brodie, J. P., Chomiuk, L., Spitler, L. R., Strader, J., Benson, A. J., & Forbes, D. A. 2011, ApJ, 736, L26

Babak, S., et al. 2017, PhRvD, 95, 103012

Balcells, M., Graham, A. W., Domnguez-Palmero, L., & Peletier, R. F. 2003, ApJ, 582, L79

Balcells, M., Graham, A. W., & Peletier, R. F. 2007, ApJ, 665, 1084

Banik, N., Tan, J. C., & Monaco, P. 2019, MNRAS, 483, 3592

Barro, G., et al. 2024, ApJ, 963, 128

Baum, W. A. 1959, PASP, 71, 106

Bean, R., & Magueijo, J. 2002, PhRvD, 66, 063505

Begelman, M. C., Blandford, R. D., & Rees, M. J. 1980, Natur, 287, 307

Begelman, M. C., Volonteri, M., & Rees, M. J. 2006, MNRAS, 370, 289

Bekki, K., Couch, W. J., & Drinkwater, M. J. 2001, ApJ, 552, L105

Bekki, K., & Freeman, K. C. 2003, MNRAS, 346, L11

Bekki, K., & Graham, A. W. 2010, ApJ, 714, L313

Bell, E. F., & de Jong, R. S. 2001, ApJ, 550, 212

Bennert, V. N., Auger, M. W., Treu, T., Woo, J.-H., & Malkan, M. A. 2011, ApJ, 742, 107

Bennert, V. N., et al. 2021, ApJ, 921, 36

Bentz, M. C., & Manne-Nicholas, E. 2018, ApJ, 864, 146

Bentz, M. C., Peterson, B. M., Pogge, R. W., & Vestergaard, M. 2009, ApJ, 694, L166

Bergvall, N., Zackrisson, E., Andersson, B. G., Arnberg, D., Masegosa, J., & Östlin, G. 2006, A&A, 448, 513

Binggeli, B., & Popescu, C. C. 1995, A&A, 298, 63

Binggeli, B., Sandage, A., & Tammann, G. A. 1985, AJ, 90, 1681

Bongiorno, A., et al. 2014, MNRAS, 443, 2077

Brodie, J. P., Romanowsky, A. J., Strader, J., & Forbes, D. A. 2011, AJ, 142, 199

Brum, C., et al. 2019, MNRAS, 486, 691

Bunker, A. J., et al. 2023, A&A, 677, A88

Busch, G., et al. 2014, A&A, 561, A140

Buta, R. J., et al. 2015, ApJS, 217, 32

Cairós, L. M., Caon, N., Papaderos, P., Noeske, K., Vlchez, J. M., Garca Lorenzo, B., & Muñoz-Tuñón, C. 2003, ApJ, 593, 312

Cairós, L. M., Vlchez, J. M., González Pérez, J. N., Iglesias-Páramo, J., & Caon, N. 2001, ApJS, 133, 321

Cameron, E., Driver, S. P., Graham, A. W., & Liske, J. 2009, ApJ, 699, 105

Cardamone, C., et al. 2009, MNRAS, 399, 1191

Carnall, A. C., et al. 2023, Natur, 619, 716

Chilingarian, I. V., Cayatte, V., & Bergond, G. 2008, MNRAS, 390, 906

Chilingarian, I. V., Katkov, I. Y., Zolotukhin, I. Y., Grishin, K. A., Beletsky, Y., Boutsia, K., & Osip, D. J. 2018, ApJ, 863, 1

Chilingarian, I. V., & Mamon, G. A. 2008, MNRAS, 385, L83

Chilingarian, I. V., Mieske, S., Hilker, M., & Infante, L. 2011, MNRAS, 412, 1627

Chilingarian, I., & Zolotukhin, I. 2015, Sci, 348, 418

Chomiuk, L., Strader, J., & Brodie, J. P. 2008, AJ, 136, 234

Ciambur, B. C., & Graham, A. W. 2016, MNRAS, 459, 1276

Conselice, C. J., Gallagher, J. S. I., & Wyse, R. F. G. 2003, AJ, 125, 66

Côté, P., et al. 2006, ApJS, 165, 57

D'Onghia, E., Vogelsberger, M., & Hernquist, L. 2013, ApJ, 766, 34

D'Souza, R., & Rix, H.-W. 2013, MNRAS, 429, 1887

Daddi, E., et al. 2005, ApJ, 626, 680

Damjanov, I., et al. 2011, ApJ, 739, L44

Damjanov, I., Hwang, H. S., Geller, M. J., & Chilingarian, I. 2014, ApJ, 793, 39

Das, A., Schleicher, D. R. G., Basu, S., & Boekholt, T. C. N. 2021, MNRAS, 505, 2186

Davies, R. D., & Lewis, B. M. 1973, MNRAS, 165, 231

Davies, M. B., Miller, M. C., & Bellovary, J. M. 2011, ApJ, 740, L42

Davis, B. L., Graham, A. W., & Cameron, E. 2018, ApJ, 869, 113

Davis, B. L., Graham, A. W., & Cameron, E. 2019, ApJ, 873, 85

Davis, T. A., et al. 2020, MNRAS, 496, 4061

De Felice, A., & Tsujikawa, S. 2010, LRR, 13, 3

de Graaff, A., et al. 2025, arXiv e-prints, p. arXiv:2503.16600

de Martino, I., Chakrabarty, S. S., Cesare, V., Gallo, A., Ostorero, L., & Diaferio, A. 2020, Universe, 6, 107

de Vaucouleurs, G. 1961, ApJS, 5, 233

de Vaucouleurs, G., & de Vaucouleurs, A. 1972, MmRAS, 77, 1

Decarli, R., et al. 2018, ApJ, 854, 97

den Brok, M., et al. 2015, ApJ, 809, 101

Devecchi, B., & Volonteri, M. 2009, ApJ, 694, 302

Ding, X., et al. 2020, ApJ, 888, 37

Ding, X., et al. 2023, Natur, 621, 51

Dolgov, A., & Postnov, K. 2017, JCAP, 2017, 036

Doroshkevich, A. G., Zel'dovich, Y. B., & Novikov, I. D. 1967, SvA, 11, 233

Dressler, A. 1989, in IAU Symposium, Vol. 134, Active Galactic Nuclei, ed. D. E. Osterbrock, & J. S. Miller (Dordrecht: Kluwer Academic Publishers), 217

Dressler, A., & Richstone, D. O. 1988, ApJ, 324, 701

Drinkwater, M. J., Gregg, M. D., Hilker, M., Bekki, K., Couch, W. J., Ferguson, H. C., Jones, J. B., & Phillipps, S. 2003, Natur, 423, 519

Drinkwater, M. J., Jones, J. B., Gregg, M. D., & Phillipps, S. 2000, PASA, 17, 227

Driver, S. P., Allen, P. D., Liske, J., & Graham, A. W. 2007, ApJ, 657, L85

Dullo, B. T., & Graham, A. W. 2014, MNRAS, 444, 2700

Eisenstein, D. J., et al. 2005, ApJ, 633, 560

Elmegreen, D. M., & Elmegreen, B. G. 2017, ApJ, 851, L44

Evrard, A. E., Summers, F. J., & Davis, M. 1994, ApJ, 422, 11

Fall, S. M., & Pei, Y. C. 1993, ApJ, 402, 479

Famaey, B., & McGaugh, S. S. 2012, LRR, 15, 10

Forbes, D. A., Ferré-Mateu, A., Durré, M., Brodie, J. P., & Romanowsky, A. J. 2020, MNRAS, 497, 765

Frank, M. J., Hilker, M., Mieske, S., Baumgardt, H., Grebel, E. K., & Infante, L. 2011, MNRAS, 414, L70

Freeman, K. C. 1993, in Astronomical Society of the Pacific Conference Series, Vol. 48, The Globular Cluster-Galaxy Connection, ed. G. H. Smith, & J. P. Brodie, 608

Furtak, L. J., et al. 2024, Natur, 628, 57

Gair, J. R., Babak, S., Sesana, A., Amaro-Seoane, P., Barausse, E., Berry, C. P. L., Berti, E., & Sopuerta, C. 2017, In Journal of Physics Conference Series (IOP), 012021 (arXiv 1704.00009), 10.1088/1742-6596/840/1/012021

Gehlbach, H., Robinson, C. D., & Fletcher, A. 2024, PLOS ONE, 19, 1

Graham, A. W. 2004, ApJ, 613, L33

Graham, A. W. 2007, MNRAS, 379, 711

Graham, A. W. 2012, ApJ, 746, 113

Graham, A. W. 2013, in Planets, Stars and Stellar Systems. Volume 6: Extragalactic Astronomy and Cosmology, ed. T. D. Oswalt, & W. C. Keel (Dordrecht: Springer Science+Business Media), 91, doi:10.1007/978-94-007-5609-0_2

Graham, A. W. 2014, in Astronomical Society of the Pacific Conference Series Vol. 480, Structure and Dynamics of Disk Galaxies, ed. M. S. Seigar, & P. Treuthardt, 185 (arXiv 1311.7207), doi:10.48550/arXiv.1311.7207

Graham, A. W. 2016, in IAU Symposium, Vol. 312, Star Clusters and Black Holes in Galaxies across Cosmic Time, ed. Y. Meiron, S. Li, F. K. Liu, & R. Spurzem, 269 (arXiv 1412.5715), doi:10.1017/S1743921315008017

Graham, A. W. 2020, MNRAS, 492, 3263

Graham, A. W. 2023a, MNRAS, 521, 1023

Graham, A. W. 2023b, MNRAS, 522, 3588

Graham, A. W. 2024a, MNRAS, 531, 230

Graham, A. W. 2024b, MNRAS, 535, 299

Graham, A. W., & Guzmán, R. 2003, AJ, 125, 2936

Graham, A. W., & Sahu, N. 2023a, MNRAS, 518, 2177

Graham, A. W., & Sahu, N. 2023b, MNRAS, 520, 1975

Graham, A. W., & Sahu, N. 2024, MNRAS, 530, 3429

Graham, A. W., & Scott, N. 2013, ApJ, 764, 151

Graham, A. W., & Scott, N. 2015, ApJ, 798, 54

Graham, A. W., & Spitler, L. R. 2009, MNRAS, 397, 2148

Graham, A. W., & Worley, C. C. 2008, MNRAS, 388, 1708

Graham, A. W., Ciambur, B. C., & Savorgnan, G. A. D. 2016b, ApJ, 831, 132

Graham, A. W., Durré, M., Savorgnan, G. A. D., Medling, A. M., Batcheldor, D., Scott, N., Watson, B., & Marconi, A. 2016a, ApJ, 819, 43

Graham, A. W., Jarrett, T. H., & Cluver, M. E. 2024, MNRAS, 527, 10059

Graham, A. W., Onken, C. A., Athanassoula, E., & Combes, F. 2011, MNRAS, 412, 2211

Graham, A. W., Spitler, L. R., Forbes, D. A., Lisker, T., Moore, B., & Janz, J. 2012, ApJ, 750, 121

Gu, H., Wu, X.-B., Wen, Y., Ma, Q., & Guo, H. 2024, MNRAS, 530, 3578

Gualandris, A., & Merritt, D. 2012, ApJ, 744, 74

Gunn, J. E., & Gott, J. R. I. 1972, ApJ, 176, 1

Guzmán, R., Östlin, G., Kunth, D., Bershady, M. A., Koo, D. C., & Pahre, M. A. 2003, ApJ, 586, L45

Haas, M. 1998, A&A, 337, L1

Häberle, M., et al. 2024, Natur, 631, 285

Hargis, J. R., Rhode, K. L., Strader, J., & Brodie, J. P. 2011, ApJ, 738, 113

Harikane, Y., et al. 2023, ApJ, 959, 39

Harris, W. E., Pritchet, C. J., & McClure, R. D. 1995, ApJ, 441, 120

Hau, G. K. T., Spitler, L. R., Forbes, D. A., Proctor, R. N., Strader, J., Mendel, J. T., Brodie, J. P., & Harris, W. E. 2009, MNRAS, 394, L97

Hilker, M., Baumgardt, H., Infante, L., Drinkwater, M., Evstigneeva, E., & Gregg, M. 2007, A&A, 463, 119

Hilker, M., Infante, L., Vieira, G., Kissler-Patig, M., & Richtler, T. 1999, A&AS, 134, 75

Hon, D. S. H., Graham, A. W., & Sahu, N. 2023, MNRAS, 519, 4651

Hopp, U., Wagner, S. J., & Richtler, T. 1995, A&A, 296, 633

Ideta, M., & Makino, J. 2004, ApJ, 616, L107

Inayoshi, K., Visbal, E., & Haiman, Z. 2020, ARA&A, 58, 27

Izumi, T., et al. 2018, PASJ, 70, 36

Izumi, T., et al. 2021, ApJ, 914, 36

Jiang, N., Ho, L. C., Dong, X.-B., Yang, H., & Wang, J. 2013, ApJ, 770, 3

Jiang, Y.-F., Greene, J. E., & Ho, L. C. 2011, ApJ, 737, L45

Julian, W. H., & Toomre, A. 1966, ApJ, 146, 810

Juodžbalis, I., et al. 2024, Natur, 636, 594

Khoperskov, A. V., Khrapov, S. S., & Sirotin, D. S. 2023, Galaxies, 12, 1

Kim, J., Park, C., L'Huillier, B., & Hong, S. E. 2015, JKAS, 48, 213

Kocevski, D. D., et al. 2023, ApJ, 954, L4

Kocevski, D. D., et al. 2025, ApJ, 986, 126

Kokorev, V., et al. 2023, ApJ, 957, L7

Kokorev, V., et al. 2024a, ApJ, 968, 38

Kokorev, V., et al. 2024b, ApJ, 975, 178

Kormendy, J., & Richstone, D. 1995, ARA&A, 33, 581

Krajnović, D., et al. 2015, MNRAS, 452, 2

Lamastra, A., Menci, N., Fiore, F., di Porto, C., & Amendola, L. 2012, MNRAS, 420, 2429

Lane, J. M. M., Bovy, J., & Mackereth, J. T. 2023, MNRAS, 526, 1209

Laor, A. 1998, ApJ, 505, L83

Laor, A. 2001, ApJ, 553, 677

Laor, A. 2006, ApJ, 643, 112

Larson, R. L., et al. 2022, ApJ, 930, 104

Larson, R. L., et al. 2023, ApJ, 953, L29

Liller, M. H. 1966, ApJ, 146, 28

Limberg, G. 2024, ApJ, 977, L2

Lin, R., et al. 2025, ApJ, 980, L34

Lin, R., et al. 2024b, SCPMA, 67, 109811

Lisker, T., Glatt, K., Westera, P., & Grebel, E. K. 2006, AJ, 132, 2432

Liu, C., et al. 2020, ApJS, 250, 17

Lotz, J. M., Telford, R., Ferguson, H. C., Miller, B. W., Stiavelli, M., & Mack, J. 2001, ApJ, 552, 572

Lyubenova, M., et al. 2013, MNRAS, 431, 3364

Madrid, J. P., et al. 2010, ApJ, 722, 1707

Magorrian, J., et al. 1998, AJ, 115, 2285

Maiolino, R., et al. 2024, A&A, 691, 145

Maiolino, R., et al. 2024, Natur, 627, 59

Mapelli, M., Ripamonti, E., Vecchio, A., Graham, A. W., & Gualandris, A. 2012, A&A, 542, A102

Marleau, F. R., et al. 2006, ApJ, 646, 929

Mateo, M., Olszewski, E. W., & Walker, M. G. 2008, ApJ, 675, 201

Mathur, S., Fields, D., Peterson, B. M., & Grupe, D. 2012, ApJ, 754, 146

Matthee, J., et al. 2024, ApJ, 963, 129

Menezes, R. B., Steiner, J. E., & Ricci, T. V. 2014, ApJ, 796, L13

Mérida, R. M., et al. 2025, arXiv e-prints, p. arXiv:2501.17925

Miller, J. S., Goodrich, R. W., & Mathews, W. G. 1991, ApJ, 378, 47

Milgrom, M. 1983, ApJ, 270, 384

Moffat, J. W. 2006, JCAP, 2006, 004

Moffett, A. J., et al. 2016, MNRAS, 457, 1308

Moffett, A. J., et al. 2019, MNRAS, 489, 2830

Molaeinezhad, A., et al. 2019, MNRAS, 488, 1012

Mowla, L., Iyer, K., & Asada, Y. 2024, Natur, 636, 332

Naidu, R. P., et al. 2025, arXiv e-prints, p. arXiv:2503.16596

Nguyen, D. D., et al. 2018, ApJ, 858, 118

Nguyen, D. D., et al. 2019, ApJ, 872, 104

Nguyen, D. D., et al. 2022, MNRAS, 509, 2920

Nieto, J. L., & Bender, R. 1989, A&A, 215, 266

Nieto, J. L., Capaccioli, M., & Held, E. V. 1988, A&A, 195, L1

Omukai, K., Schneider, R., & Haiman, Z. 2008, ApJ, 686, 801

Onken, C. A., Ferrarese, L., Merritt, D., Peterson, B. M., Pogge, R. W., Vestergaard, M., & Wandel, A. 2004, ApJ, 615, 645

Pandey, S., et al. 2024, ApJ, 976, 116

Park, D., Woo, J.-H., Bennert, V. N., Treu, T., Auger, M. W., & Malkan, M. A. 2015, ApJ, 799, 164

Pascale, R., Nipoti, C., Calura, F., & Della Croce, A. 2024, A&A, 684, L19

Paudel, S., Hilker, M., Ree, C. H., & Kim, M. 2016, ApJ, 820, L19

Pechetti, R., et al. 2022, ApJ, 924, 48

Pensabene, A., Carniani, S., Perna, M., Cresci, G., Decarli, R., Maiolino, R., & Marconi, A. 2020, A&A, 637, A84

Percival, W. J., Cole, S., Eisenstein, D. J., Nichol, R. C., Peacock, J. A., Pope, A. C., & Szalay, A. S. 2007, MNRAS, 381, 1053

Pérez-Gallego, J., et al. 2011, MNRAS, 418, 2350

Pérez-González, P. G., et al. 2024, ApJ, 968, 4

Peterson, B. M. 1993, PASP, 105, 247

Pfeffer, J., & Baumgardt, H. 2013, MNRAS, 433, 1997

Phillipps, S., Disney, M. J., Kibblewhite, E. J., & Cawson, M. G. M. 1987, MNRAS, 229, 505

Phillipps, S., Drinkwater, M. J., Gregg, M. D., & Jones, J. B. 2001, ApJ, 560, 201

Poci, A., McDermid, R. M., Zhu, L., & van de Ven, G. 2019, MNRAS, 487, 3776

Portegies Zwart, S. F., & McMillan, S. L. W. 2002, ApJ, 576, 899

Preto, M., & Amaro-Seoane, P. 2010, ApJ, 708, L42

Randall, S. W., et al. 2015, ApJ, 805, 112

Reaves, G. 1983, ApJS, 53, 375

Reines, A. E., Greene, J. E., & Geha, M. 2013, ApJ, 775, 116

Reines, A. E., & Volonteri, M. 2015, ApJ, 813, 82

Richings, A. J., Uttley, P., & Kording, E. 2011, MNRAS, 415, 2158

Rinaldi, P., et al. 2024, arXiv e-prints, p. arXiv:2411.14383

Romanishin, W., Strom, K. M., & Strom, S. E. 1977, BAAS, 347

Rusakov, V., et al. 2025, arXiv e-prints, p. arXiv:2503.16595

Rusli, S. P., Thomas, J., Erwin, P., Saglia, R. P., Nowak, N., & Bender, R. 2011, MNRAS, 410, 1223

Ryu, T., Tanaka, T. L., Perna, R., & Haiman, Z. 2016, MNRAS, 460, 4122

Sahu, N., Graham, A. W., & Davis, B. L. 2019, ApJ, 876, 155

Sahu, N., Graham, A. W., & Davis, B. L. 2020, ApJ, 903, 97

Sahu, N., Graham, A. W., & Hon, D. S. H. 2023, MNRAS, 518, 1352

Salucci, P., Ratnam, C., Monaco, P., & Danese, L. 2000, MNRAS, 317, 488

Sandage, A., Binggeli, B., & Tammann, G. A. 1985, AJ, 90, 1759

Saulder, C., van den Bosch, R. C. E., & Mieske, S. 2015, A&A, 578, A134

Savorgnan, G. A. D., & Graham, A. W. 2016a, ApJS, 222, 10

Savorgnan, G. A. D., & Graham, A. W. 2016b, MNRAS, 457, 320

Savorgnan, G. A. D., Graham, A. W., Marconi, A., & Sani, E. 2016, ApJ 817, 21

Sawangwit, U., Shanks, T., Abdalla, F. B., Cannon, R. D., Croom, S. M., Edge, A. C., Ross, N. P., & Wake, D. A. 2011, MNRAS, 416, 3033

Schawinski, K., et al. 2014, MNRAS, 440, 889

Schindler, J.-T., et al. 2024, arXiv e-prints, p. arXiv:2411.11534

Schmidt, M. 1963, Natur, 197, 1040

Scorza, C., & Bender, R. 1995, A&A, 293, 20

Scorza, C., & van den Bosch, F. C. 1998, MNRAS, 300, 469

Scott, N., Graham, A. W., & Schombert, J. 2013, ApJ, 768, 76

Serra, P., et al. 2019, A&A, 628, A122

Seth, A. C., et al. 2014, Natur, 513, 398

Shankar, F., et al. 2016, MNRAS, 460, 3119

Shao, Y., et al. 2017, ApJ, 845, 138

Shi, F., Kong, X., Li, C., & Cheng, F. Z. 2005, A&A, 437, 849

Sil'chenko, O. 2013, Memorie della Societa Astronomica Italiana Supplementi, 25, 93

Sil'chenko, O. K., Afanasiev, V. L., Chavushyan, V. H., & Valdes, J. R. 2002, ApJ, 577, 668

Spaans, M., & Silk, J. 2006, ApJ, 652, 902

Stickel, M., Rieke, G. H., Kuehr, H., & Rieke, M. J. 1996, ApJ, 468, 556

Suh, H., et al. 2025, NatAs, 9, 271

Tan, J. C., Singh, J., Cammelli, V., Sanati, M., Petkova, M., Nandal, D., & Monaco, P. 2024, arXiv e-prints, p. arXiv:2412.01828

Taylor, M. A., et al. 2025, arXiv e-prints, p. arXiv:2503.00113

Tripodi, R., et al. 2024, arXiv e-prints p. arXiv:2412.04983

Trujillo, I., Ferré-Mateu, A., Balcells, M., Vazdekis, A., & Sánchez-Blázquez, P. 2014, ApJ, 780, L20

Übler, H., et al. 2023, A&A, 677, A145

Umemura, M., Loeb, A., & Turner, E. L. 1993, ApJ, 419, 459

van den Bosch, R. C. E., Gebhardt, K., Gültekin, K., van de Ven, G., van der Wel, A., & Walsh, J. L. 2012, Natur, 491, 729

van Dokkum, P. G., et al. 2008, ApJ, 677, L5

Venemans, B. P., Walter, F., Zschaechner, L., Decarli, R., De Rosa, G., Findlay, J. R., McMahon, R. G., & Sutherland, W. J. 2016, ApJ, 816, 37

Vestergaard, M., & Peterson, B. M. 2006, ApJ, 641, 689

Volonteri, M., & Rees, M. J. 2005, ApJ, 633, 624

Walsh, J. L., van den Bosch, R. C. E., Gebhardt, K., Yildirim, A., Gültekin, K., Husemann, B., & Richstone, D. O. 2015, ApJ, 808, 183

Wandel, A. 1999, ApJ, 519, L39

Wang, R., et al. 2010, ApJ, 714, 699

Wang, R., et al. 2013, ApJ, 773, 44

Wang, R., et al. 2016, ApJ, 830, 53

Wang, B., et al. 2024, ApJ, 969, L13

Webster, R. L., Francis, P. J., Petersont, B. A., Drinkwater, M. J., & Masci, F. J. 1995, Natur, 375, 469

Willott, C. J., Bergeron, J., & Omont, A. 2015, ApJ, 801, 123

Willott, C. J., Bergeron, J., & Omont, A. 2017, ApJ, 850, 108

Wolf, C., Lai, S., Onken, C. A., Amrutha, N., Bian, F., Hon, W. J., Tisserand, P., & Webster, R. L. 2024, NatAs, 8, 520

Yldrm, A., van den Bosch, R. C. E., van de Ven, G., Husemann, B., Lyubenova, M., Walsh, J. L., Gebhardt, K., & Gültekin, K. 2015, MNRAS, 452, 1792

Yuan, W., Zhou, H., Dou, L., Dong, X. B., Fan, X., & Wang, T. G. 2014, ApJ, 782, 55

Yue, M., Eilers, A.-C., Ananna, T. T., Panagiotou, C., Kara, E., & Miyaji, T. 2024, ApJ, 974, L26

Zinnecker, H., Keable, C. J., Dunlop, J. S., Cannon, R. D., & Griffiths, W. K. 1988, in IAU Symposium, Vol. 126, The Harlow-Shapley Symposium on Globular Cluster Systems in Galaxies, ed. J. E. Grindlay, & A. G. D. Philip, 603

Zwicky, F., & Kowal, C. T. 1968, "Catalogue of Galaxies and of Clusters of Galaxies", Volume VI (Pasadena: California Institute of Technology)

Zwicky, F., & Zwicky, M. A. 1971, Catalogue of Selected Compact Galaxies and of Post-Eruptive Galaxies, Guemligen, Switzerland